# OPTIMIZATION OF THE DISCHARGE VALVE TO INCREASE ITS FLOW CAPACITY

**IVAN MIHALIK[1], TOMAS BRESTOVIC[1],**

**MARIAN LAZAR[1], NATALIA JASMINSKA[1]**

[1]Department of Energy Engineering, Faculty of Mechanical Engineering, Technical University of Kosice, Slovakia

**DOI: 10.17973/MMSJ.2025_12_2025088**

**Ivan.mihalik@tuke.sk**

The article describes the original state of the discharge valve design in terms of geometry and flow conditions. Through the simulations performed, it shows in detail the velocity and pressure fields in the valve in individual time steps of the liquid discharge process. By combining numerical and analytical calculations, it determines the total liquid flow through the valve during a specified time interval, while based on the knowledge gained, it suggests changes to the valve geometry to optimize the liquid flow. Key geometry modifications include the elimination of various sharp edges of individual elements of the original design but also limiting the maximum valve extension distance in the open mode. Performing the calculation for the optimized shape demonstrated a significant improvement in the valve flow properties compared to the original variant by 49% during the first second, or 52% during the first 2 seconds after opening the valve.

**KEYWORDS**

valve, fluid flow, optimization, CFD

## 1 INTRODUCTION

Some devices need to achieve a specified flow rate of liquid medium at a certain moment to ensure the proper operation of various systems. Given that hydraulic systems are an integral part of many devices, the design and optimization of key hydraulic components are long-term important engineering topics, with several studies dealing with the optimization of various types of valves. Filo et al. addressed the design and flow analysis of an adjustable check valve using CFD method [Filo 2021]. Their main goal was to properly shape and arrange holes and flow channels inside the body, between the cartridge valve and the connecting plate. Modifications of the check valve resulted in a decrease of maximum fluid flow velocity by approximately 30%, and pressure loss has been decreased by 30–40%. Shi et al. addressed the structural optimization and mechanical property analysis of butterfly valves, while managing to reduce the local resistance coefficient by 52.74% [Shi 2025].

A frequent subject of optimization is, for example, spool valves. Research on and optimization of the flow force of hydraulic spool valves was carried out, for example, by Li et al., focusing on calculation methods, influencing factors, and methods for reducing the flow force of slide valves [Li 2023]. Frosina et al. created mathematical model to analyze the torque caused by fluid-solid interaction on a hydraulic valve, while models were also validated by experimental data [Frosina 2015]. Olivetti et al. published paper to show how a completely virtual optimization approach is useful to design new geometries in order to improve the performance of valves [Olivetti 2020]. Experimental validation of sliding spool design for reducing the actuation forces in directly operated proportional directional valves was performed by Amirante et al. to extend the application range of these valves to higher values of pressure and flow rate [Amirante 2016]. Yang et al. optimized miniature switching valve using Ansys Fluent to achieve the reduction of power consumption [Yang 2024]. Optimized design of the spool in an electro-hydraulic proportional directional valve proposed by Chen et al. reduced turbulent kinetic energy by 38.7% [Chen 2025].

The examined discharge valve is not continuously open during operation but is intended to provide a sufficient amount of water within a short time from the moment of its opening. The valve is then closed. Ensuring the correct flow rate can be problematic in specific cases depending on the length of the supply pipe and the position of the device. A possible solution is the application of a pressure tank near the device. This tank ensures the delivery of the necessary amount of liquid in a set time, while the pressure in the tank depends on the volume of air in the tank. Gas expansion depends on the type of thermodynamic change performed by the air. Despite the fact that the course of this change is polytropic, to simplify the calculation, due to the relatively small change in volume over time and negligible heat transfer between the wall and the air, it is possible to consider an isothermal change.

## 2 TERMODYNAMIC DESCRIOTION OF AIR EXPANSION IN A TANK

When initially filling a tank with an initial atmospheric pressure and a volume of $6 \cdot 10^{-3}$ m³, the air is compressed to the operating pressure of 350 kPa. When considering an isothermal change, it is possible to determine the volume to which the air in the reservoir is compressed by modifying the Boyle-Mariotte law:

$$V_1 = \frac{p_0 \cdot V_0}{p_1} \quad (\mathrm{m}^3) \tag{1}$$

where $V_1$ is the volume of air in the tank after compression (m³), $V_0$ – total tank volume (m³), $p_1$ – absolute operating pressure (Pa), $p_0$ – atmospheric pressure in the tank before compression (Pa).

The relationship between volume and pressure can be expressed through the following differential equation:

$$\mathrm{d}V = -\frac{p_1 \cdot V_1}{p^2} \cdot \mathrm{d}p \quad (\mathrm{m}^3) \tag{2}$$

where $p$ is the air pressure at time $\tau$ (Pa).

The elementary change in air volume can be expressed as the difference in liquid flow rates at the inlet and outlet of the tank:

$$\mathrm{d}V = (Q_{\mathrm{V2}} - Q_{\mathrm{V1}}) \cdot \mathrm{d}\tau = \frac{Q_{\mathrm{m2}} - Q_{\mathrm{m1}}}{\rho} \cdot \mathrm{d}\tau \quad (\mathrm{m}^3) \tag{3}$$

where $Q_{\mathrm{V2}}$ is the immediate volumetric flow rate at the outlet of the tank (m³·s⁻¹), $Q_{\mathrm{V1}}$ – immediate volumetric flow rate at the inlet of the tank (m³·s⁻¹), dτ – elementary change in time (s), $Q_{\mathrm{m2}}$ – immediate mass flow rate at the outlet of the tank (kg·s⁻¹), $Q_{\mathrm{m1}}$ – immediate mass flow rate at the inlet of the tank (kg·s⁻¹), $\rho$ – water density (kg·m⁻³).

The result of combining equations (2) and (3) is the differential equation (4):

$$\frac{Q_{\mathrm{m2}} - Q_{\mathrm{m1}}}{\rho} \cdot \mathrm{d}\tau = -\frac{p_1 \cdot V_1}{p^2} \cdot \mathrm{d}p \quad (\mathrm{m}^3) \tag{4}$$

The solution of this equation (4) is possible only if the dependencies of the variables on pressure and time are known. The determination of the flow rate at the outlet of the tank, which is a function of pressure and time, is particularly problematic. Since the flow of the liquid depends on the geometry of the valve, it is necessary to perform a numerical calculation using the finite volume method. Since a definite analytical calculation of equation (4) is not possible, it is necessary to modify it to the form:

$$\Delta p = -\frac{(Q_{m2} - Q_{m1}) \cdot p^2}{\rho \cdot p_1 \cdot V_1} \cdot \Delta\tau \quad \text{(Pa)} \tag{5}$$

The inlet flow rate $Q_{m1}$ depends on the total coefficient of local and length losses resulting from the shape and length of the supply pipe. The calculation assumes that the maximum inlet flow rate $Q_{m1}$ is 0.5 kg·s$^{-1}$. This flow rate is achieved with an empty tank with an absolute pressure of 101.325 kPa and an external system pressure of 350 kPa.

The pressure difference between the main water pipe and the tank will cause an inflow of water with a mass flow rate of $Q_{m1}$. The basic relationship describing the pressure losses in pipes at a known water velocity is expressed as:

$$p_1 - p = \sum\zeta \cdot \frac{v^2}{2} \cdot \rho \quad \text{(Pa)} \tag{6}$$

where $\Sigma\zeta$ is the total equivalent coefficient of local and longitudinal losses of the supply pipe (-), $v$ – water velocity in the supply pipe (m·s$^{-1}$).

By modifying relation (6) we obtain:

$$p_1 - p = \sum\zeta \cdot \frac{Q_{m1}^2}{2 \cdot S_1^2 \cdot \rho} \quad \text{(Pa)} \tag{7}$$

where $S_1$ is the internal cross-sectional area of the supply pipe (m$^2$).

By introducing the substitution $k$, it is possible to calculate the actual flow rate at a known tank operating pressure:

$$k = \frac{\sum\zeta}{S_1^2} = \frac{2 \cdot \rho \cdot (p_1 - p_0)}{Q_{m1-Ini}^2} = 2 \cdot 10^9 \ \text{(m}^{-4}\text{)} \tag{8}$$

where Qm1-Ini is the initial water flow rate when filling the tank and the pressure is 101,325 Pa (kg·s$^{-1}$).

$$Q_{m1}^2 = \sqrt{\frac{2 \cdot \rho \cdot (p_1 - p)}{k}} \ \text{(kg} \cdot \text{s}^{-1}\text{)} \tag{9}$$

By gradually alternating numerical and analytical calculations, it is possible to obtain the flow, pressure and volume curves as a function of time.

## 3 ORIGINAL DISCHARGE VALVE DESIGN

The opening and closing cycle of the original valve takes a total of 4 seconds. The valve opens for 0.3 seconds, the valve is fully open for 1.7 seconds and then closes for 2 seconds. The overpressure during the valve opening fluctuates slightly, but its average value is 0.25 MPa. The liquid temperature is 10 °C. The original valve geometry is shown in Fig. 1. The valve displacement during its opening is 10 mm.

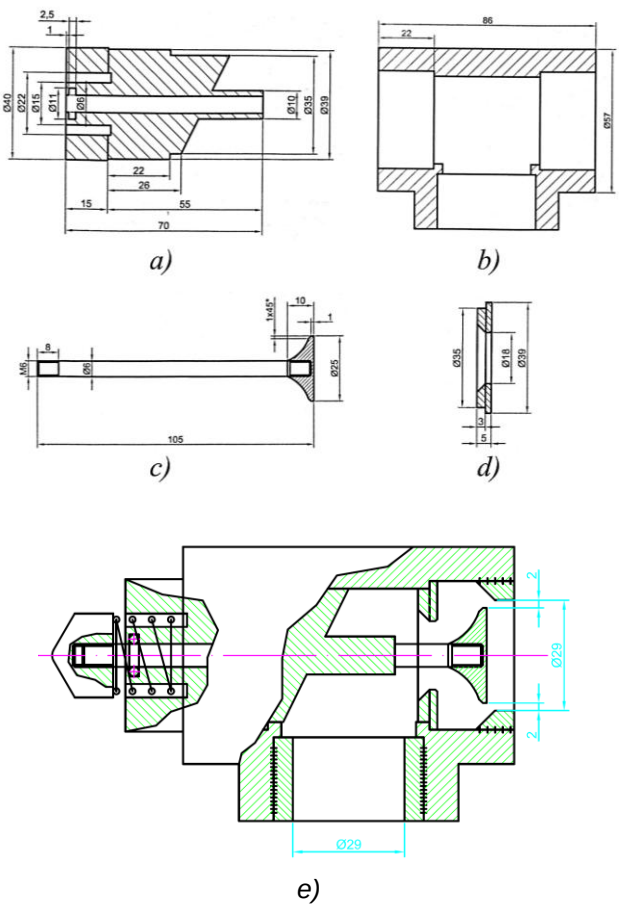


**Figure 1.** a) Original valve guide; b) Original valve body; c) Original valve; d) Original valve seat; e) Composite valve.

The numerical solution was implemented using the geometric symmetry of the 3D valve model, which halved the simulation time. When discrediting the body using a mesh, it was necessary to create the densest mesh possible in the area near the valve walls, where the largest velocity changes can be expected. The Tetrahedrons mesh method was used, since this method allows the application of a boundary layer (Lecheler 2022). The primary average size of the mesh elements was set to 1 mm. On selected surfaces of the body, the mesh was densified to an element size of 0.4 mm (valve and valve guide part). The size of the elements on the leading edge of the valve seat was set to 0.05 mm.

Near the walls, a boundary layer was set with respect to the used SST turbulence model. A total of 8 layers were created with an increase in thickness by a coefficient of 1.1. When changing the boundary conditions at the time of opening and closing the valve, it is necessary to change its displacement with simultaneous meshing of the geometry. In the time interval 0.3 to 2 seconds, it is not necessary to re-mesh the geometry, but it is sufficient to change only the boundary conditions. Fig. 2 shows a body with a created mesh with the number of elements of 1.76 million, while the number of elements varies slightly during the simulation depending on the valve displacement.

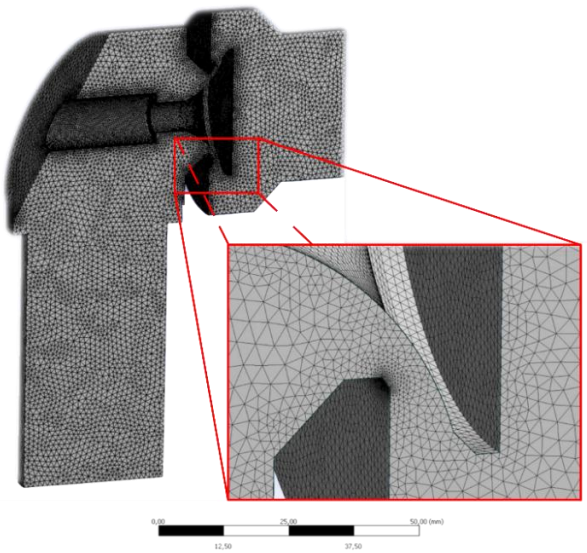

**Figure 2.** Detail of the created mesh on the original valve geometry.

The influence of the mesh size on the overall accuracy of the water flow calculation was performed for a valve opening of 10 mm at a time of 1 s after the valve opening. Four numerical solutions were created for a total mesh size of 1.56, 3.14, 6.59 and 9.08 million elements. The reference value was a mesh size of 3.14 million elements, while Fig. 3 shows the deviation of the calculated water flow depending on the number of elements.

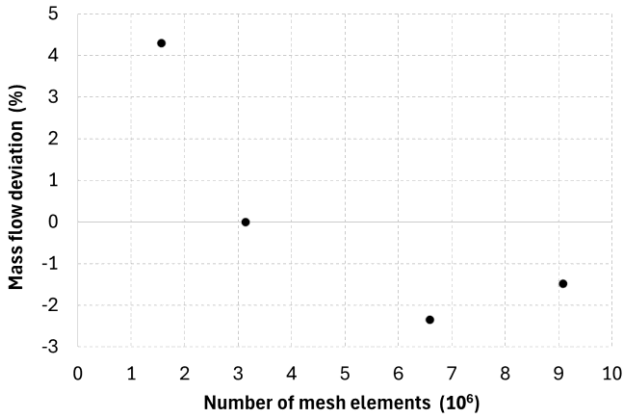


**Figure 3.** Comparison of deviations of calculated water flow depending on the number of elements.

From the numerical solution it is clear that increasing the mesh size above 3.14 million elements no longer has a significant impact on the accuracy of the calculation, but it significantly affects the length and complexity of the calculation.

The relative pressure at the inlet was set according to the iterative procedure, with the initial iteration starting with a relative pressure of 250 kPa. The relative static pressure at the outlet was 0 kPa. The number of iterations of one simulation step was 1,000 with an iterative accuracy of $10^{-6}$.

Due to the iterative solution between numerical and analytical calculations, a total of 20 simulations were performed using CFD software in the original valve geometry design. Fig. 4 shows the velocity fields at selected important specific valve positions.

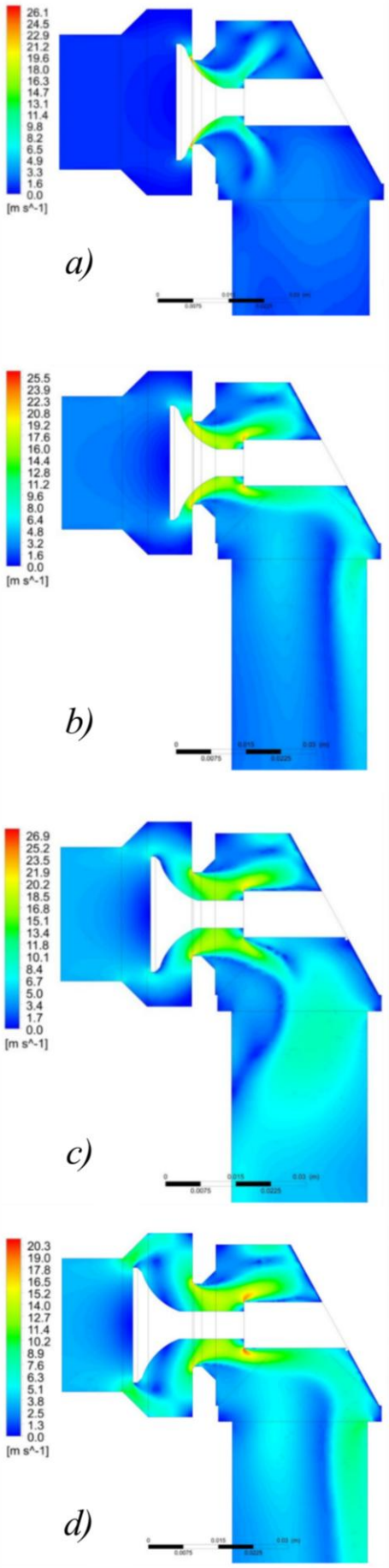


**Figure 4.** Velocity field in the plane of symmetry of the original geometry when the valve is opened to: a) 0.5 mm; b) 2 mm; c) 6 mm; d) 10 mm.

Fig. 5 shows the pressure fields of the same selected simulation specific valve positions as in the case of the velocity fields in Fig. 4.

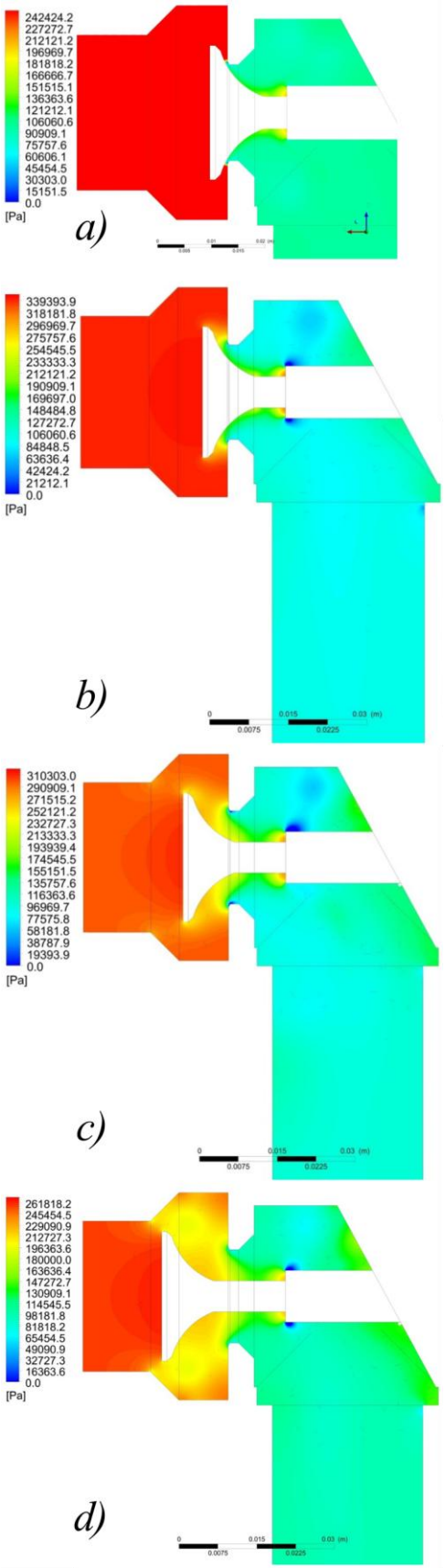


**Figure 5.** Pressure field in the plane of symmetry of the original geometry when the valve is opened to: a) 0.5 mm; b) 2 mm; c) 6 mm; d) 10 mm.

Fig. 4 a) shows the velocity field in the plane of symmetry of the valve when it is partially opened to 0.5 mm, while there is a significant curvature of the flow trajectory due to the leading edge of the guiding part. This sudden change in the flow direction causes a decrease in the flow rate through the valve, since the pressure loss is determined by the pressure difference in front of and behind the valve. The shape of the leading edge is responsible for the increase in pressure in the yellow area in Fig. 5 a), while when the valve is partially opened to 2 mm, a significant drop in pressure below the saturated vapor pressure value, which for a liquid at a given temperature represents a value of 1,227 Pa (Wexler 1976), can be observed in the blue area in Fig. 5 b). In these areas, steam bubbles subsequently form, which, due to the high flow velocity, quickly disappear after passing to an area with higher pressure. This results in the formation of cavitation, which has an adverse effect on the discharge valve and can significantly shorten its service life. At the same time, this phenomenon is accompanied by increased noise of the device. As the valve distance increases, the liquid flow rate increases, while the pressure in the tank gradually decreases.

Fig. 4 c) shows the velocity field in the plane of symmetry of the valve when it is partially opened to 6 mm. The highest flow velocities are achieved in the areas shown in red behind the sharp edges of the geometry. At a given valve opening, low-pressure areas shown in blue in Fig. 5 c) are formed even in close proximity to the valve seats. At the same time, a pressure drop can also be observed at the leading edge of the valve.

It is clear from Fig. 4 d) that when the valve is opened to a maximum distance of 10 mm, the cross-sectional area through which the liquid flows near the leading edge of the valve will be significantly reduced. This results in a decrease in flow rate.

The results of the iterative calculation for individual time steps during valve opening are shown in Tab. 1.

From the data in Tab. 1 it is clear that after opening the valve, the air in the tank expands, which results in a pressure drop. When the valve opening distance increases, it is initially possible to observe an increase in the flow rate from the tank up to a displacement value of 6 mm. After exceeding this value due to the reduction of the flow cross-section, the flow rate at the outlet from the tank decreases. After reaching a maximum displacement of 10 mm, despite maintaining the same flow cross-section, the flow rate continues to decrease due to a continuous pressure drop. The total volume of liquid flowed in a specified time can be calculated using the equation:

$$V_{\text{total}} = \frac{1\,000}{\rho} \cdot \int_0^{\tau} Q_{\text{m2}}\,\mathrm{d}\tau \quad \text{(l)} \tag{10}$$

The calculation of the original geometry was performed only during the time interval during the valve opening and while the valve remained in the open state.

| Valve displacement (mm) | $T$ (s) | $p_{abs}$ (Pa) | $V$ (l) | $Q_{m1}$ (kg·s$^{-1}$) | $Q_{m2}$ (kg·s$^{-1}$) | $\Delta\tau$ (s) | $\Delta p$ (Pa) | $V_T$ (l) | $V_{total}$ (l) |
|---|---|---|---|---|---|---|---|---|---|
| 0.2 | 0.006 | 350,000 | 1.737 | 0 | 0.335 | 0.006 | -405 | 0.002 | 0.002 |
| 0.5 | 0.015 | 349,595 | 1.739 | 0.02 | 0.62 | 0.009 | -1,085 | 0.006 | 0.008 |
| 1 | 0.03 | 348,510 | 1.744 | 0.039 | 1.093 | 0.015 | -3,160 | 0.016 | 0.024 |
| 2 | 0.06 | 345,351 | 1.76 | 0.068 | 1.773 | 0.03 | -10,031 | 0.053 | 0.077 |
| 4 | 0.12 | 335,319 | 1.813 | 0.121 | 2.545 | 0.06 | -26,901 | 0.153 | 0.23 |
| 6 | 0.18 | 308,418 | 1.971 | 0.204 | 2.902 | 0.06 | -25,332 | 0.174 | 0.404 |
| 8 | 0.24 | 283,087 | 2.148 | 0.259 | 2.746 | 0.06 | -19,668 | 0.165 | 0.569 |
| 10 | 0.3 | 263,418 | 2.308 | 0.294 | 2.293 | 0.06 | -13,685 | 0.138 | 0.706 |
| 10 | 0.4 | 249,734 | 2.434 | 0.317 | 2.184 | 0.1 | -19,160 | 0.218 | 0.925 |
| 10 | 0.5 | 230,574 | 2.637 | 0.346 | 2.046 | 0.1 | -14,871 | 0.205 | 1.129 |
| 10 | 0.6 | 215,703 | 2.818 | 0.366 | 1.911 | 0.1 | -11,822 | 0.191 | 1.32 |
| 10 | 0.7 | 203,881 | 2.982 | 0.382 | 1.814 | 0.1 | -9,789 | 0.181 | 1.502 |
| 10 | 0.8 | 194,091 | 3.132 | 0.395 | 1.724 | 0.1 | -8,237 | 0.172 | 1.674 |
| 10 | 0.9 | 185,854 | 3.271 | 0.405 | 1.647 | 0.1 | -7,055 | 0.165 | 1.839 |
| 10 | 1 | 178,799 | 3.4 | 0.414 | 1.577 | 0.1 | -6,118 | 0.158 | 1.997 |
| 10 | 1.2 | 166,563 | 3.65 | 0.428 | 1.451 | 0.2 | -9,334 | 0.29 | 2.287 |
| 10 | 1.4 | 157,229 | 3.867 | 0.439 | 1.349 | 0.2 | -7,400 | 0.27 | 2.557 |
| 10 | 1.6 | 149,829 | 4.058 | 0.447 | 1.257 | 0.2 | -5,980 | 0.251 | 2.808 |
| 10 | 1.8 | 143,849 | 4.226 | 0.454 | 1.177 | 0.2 | -4,925 | 0.235 | 3.044 |
| 10 | 2 | 138,925 | 4.376 | 0.459 | 1.111 | 0.2 | -4,140 | 0.222 | 3.266 |

**Table 1.** Results of numerical and analytical calculation of the original geometry.

where $p_{abs}$ is the absolute pressure in the tank at the inlet to the valve, $V$ – volume of air in the tank, $\Delta\tau$ – time between two simulations, $\Delta p$ – change in pressure in the tank between two simulations, $V_T$ – volume of liquid flowed through the valve between two simulations, $V_{total}$ – total volume of liquid flowed through the valve since opening.

## 4 OPTIMIZED DISCHARGE VALVE DESIGN

From the simulation results in Chapter 3 it is obvious that in the original design, when the flowing water hits the leading edge of the guide part, significant pressure gradients arise. For this reason, it is necessary to modify the geometry so that the conical part shown in blue behind the leading edge is tangentially connected to the rounded part shown in red in Fig. 6 a).

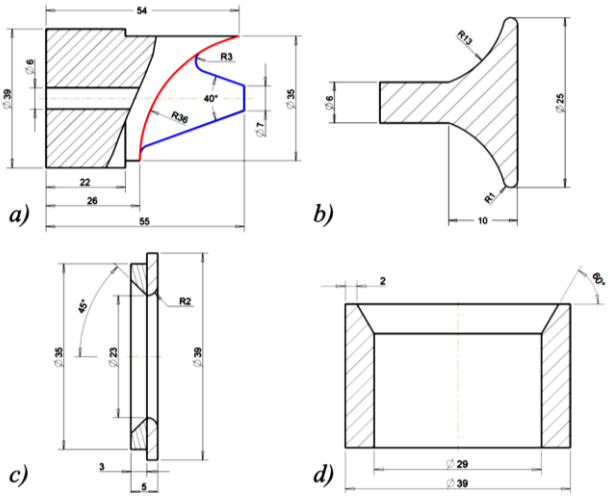


**Figure 6.** a) Modified valve guide; b) Modified valve; c) Modified valve seat; d) Modified valve body outlet pipe.

This modification will prevent sudden changes in the flow trajectory, which cause pressure gradients. By rounding the red part of the geometry, it is possible to achieve a smoother change in the flow direction in the direction perpendicular to the axis. The diameter of the leading edge is only 1 mm larger than the diameter of the piston on which the valve is located. This minimizes the pressure loss during water flow. To achieve a higher flow rate, it is not necessary to change the diameter of the valve itself, but it is appropriate to adjust the original sharp edges at its ends so that a rounding with radius R1 is created, shown in Fig. 6 b).

However, adjusting the geometry of the valve edges does not have a significant impact on the overall flow rate, since the fluid flow near the leading edge occurs at a larger diameter with lower velocities. A more fundamental improvement in the flow properties can be achieved by significantly changing the geometry of the valve seat. Rounding the original edge with a radius of R2 in Fig. 6 c) will reduce the contraction of the fluid flow and at the same time partially reduce the cavitation effect. Enlarging the internal opening of the valve seat will in turn increase the overall pressure force. Further improvement in the flow trajectory can be achieved by adjusting the outlet pipe of the valve body with an internal bevel at an angle of 60° (Fig. 5 d). This adjustment will contribute to increasing the fluid flow rate.

The modification of the geometry according to Fig. 6 will allow an increase in the total flow rate, especially in the first second after the valve is opened. Based on the simulation of the original geometry, after the valve extension distance exceeds 6 mm, the liquid flow rate starts to decrease. Therefore, at first glance, the optimal maximum valve extension distance seems to be 6 mm. However, due to the modification of the valve seat geometry, this value can be slightly increased, so the maximum valve opening was considered to be 7 mm.

The model mesh was created on a body corresponding to the internal volume of flowing water with a size of basic elements

of 1 mm. The mesh density was implemented considering the results of simulations of the original geometry in places where high pressure gradients were achieved. The mesh was also denser in the area of the surface that is in contact with the valve guide part. The total number of elements in the modified geometry exceeds 5.4 million elements for all valve displacements to achieve the most accurate results. The change of the mesh in the individual steps of the simulation is necessary when changing the valve displacement, i.e. in the interval 0 – 0.3 seconds during the valve opening and in the interval 2 – 4 seconds during the valve closing. The unambiguity conditions are identical to the simulation of the original valve geometry, and in this case, too, an iterative approach of numerical and analytical calculation is used. The calculation results for the optimized valve design are shown in Tab. 2.

| Valve displacement (mm) | $T$ (s) | $p_{abs}$ (Pa) | $V$ (l) | $Q_{m1}$ (kg·s$^{-1}$) | $Q_{m2}$ (kg·s$^{-1}$) | $\Delta\tau$ (s) | $\Delta p$ (Pa) | $V_T$ (l) | $V_{total}$ (l) |
|---|---|---|---|---|---|---|---|---|---|
| 0.2 | 0.006 | 350,000 | 1.737 | 0 | 0.459 | 0.006 | -555 | 0.003 | 0.003 |
| 0.5 | 0.015 | 349,445 | 1.740 | 0.024 | 1.208 | 0.009 | -2,141 | 0.011 | 0.014 |
| 1 | 0.03 | 347,304 | 1.750 | 0.052 | 2.362 | 0.015 | -6,876 | 0.035 | 0.049 |
| 2 | 0.06 | 340,428 | 1.786 | 0.098 | 3.743 | 0.03 | -20,847 | 0.112 | 0.161 |
| 3 | 0.09 | 319,581 | 1.902 | 0.174 | 4.352 | 0.03 | -21,056 | 0.131 | 0.292 |
| 4 | 0.12 | 298,524 | 2.037 | 0.227 | 4.6 | 0.03 | -19,231 | 0.138 | 0.43 |
| 5 | 0.15 | 279,293 | 2.177 | 0.266 | 4.658 | 0.03 | -16,906 | 0.14 | 0.57 |
| 6 | 0.18 | 262,387 | 2.317 | 0.296 | 4.565 | 0.03 | -14,504 | 0.137 | 0.707 |
| 7 | 0.21 | 247,883 | 2.453 | 0.32 | 4.428 | 0.03 | -12,457 | 0.133 | 0.839 |
| 7 | 0.3 | 210,511 | 2.888 | 0.373 | 3.817 | 0.09 | -22,589 | 0.344 | 1.183 |
| 7 | 0.4 | 187,922 | 3.235 | 0.403 | 3.394 | 0.1 | -17,374 | 0.339 | 1.522 |
| 7 | 0.5 | 170,548 | 3.565 | 0.424 | 3.03 | 0.1 | -12,469 | 0.303 | 1.825 |
| 7 | 0.6 | 158,079 | 3.846 | 0.438 | 2.74 | 0.1 | -9,462 | 0.274 | 2.099 |
| 7 | 0.7 | 148,616 | 4.091 | 0.449 | 2.499 | 0.1 | -7,450 | 0.25 | 2.349 |
| 7 | 0.8 | 141,166 | 4.307 | 0.457 | 2.292 | 0.1 | -6,014 | 0.229 | 2.578 |
| 7 | 0.9 | 135,152 | 4.498 | 0.464 | 2.111 | 0.1 | -4,949 | 0.211 | 2.79 |
| 7 | 1 | 130,203 | 4.669 | 0.469 | 1.95 | 0.1 | -4,129 | 0.195 | 2.984 |
| 7 | 1.2 | 121,945 | 4.985 | 0.478 | 1.648 | 0.2 | -5,725 | 0.33 | 3.314 |
| 7 | 1.4 | 116,219 | 5.231 | 0.484 | 1.403 | 0.2 | -4,085 | 0.281 | 3.595 |
| 7 | 1.6 | 112,135 | 5.422 | 0.488 | 1.2 | 0.2 | -2,946 | 0.24 | 3.835 |
| 7 | 1.8 | 109,188 | 5.568 | 0.491 | 1.033 | 0.2 | -2,125 | 0.207 | 4.041 |
| 7 | 2 | 107,063 | 5.678 | 0.493 | 0.896 | 0.2 | -1,518 | 0.179 | 4.22 |
| 5.25 | 2.5 | 103,268 | 5.887 | 0.497 | 0.557 | 0.5 | -529 | 0.279 | 4.499 |
| 3.5 | 3 | 102,739 | 5.917 | 0.497 | 0.439 | 0.5 | 505 | 0.22 | 4.718 |
| 1.75 | 3.5 | 103,244 | 5.888 | 0.497 | 0.327 | 0.5 | 1,485 | 0.164 | 4.882 |
| 0.2 | 4 | 104,729 | 5.805 | 0.495 | 0.001 | 0.5 | 4,460 | 0.082 | 4.964 |

**Table 2.** Results of numerical and analytical calculations of the modified geometry.

Fig. 7 shows the volume of air in the tank with the modified geometry as a function of time, in contrast to the original geometry.

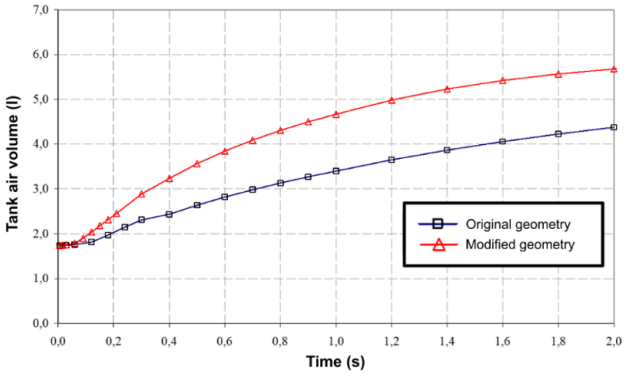


**Figure 7.** Comparison of the original and modified geometry – dependence of the air volume on time.

Fig. 7 shows a faster air expansion, which also results in a faster pressure drop in the tank, shown in Fig. 8.

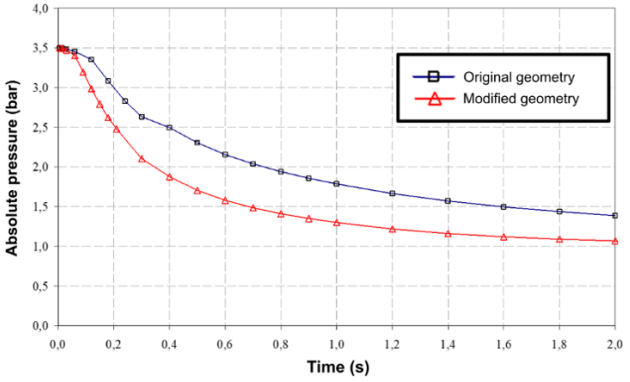


**Figure 8.** Comparison of the original and modified geometry – dependence of the absolute pressure on time.

This more significant pressure drop causes an increase in the flow of liquid into the tank (Fig. 9) compared to the original valve variant.

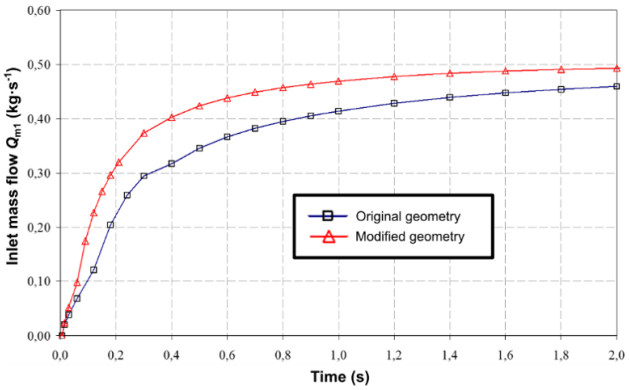


**Figure 9.** Comparison of the original and modified geometry – dependence of the flow rate into the tank on time.

To achieve the correct operating parameters of the device, the flow rate at the outlet from the tank is particularly crucial. Fig. 10 shows that the modification of the valve geometry results in a significant increase in the immediate flow rate, especially in the initial phase of opening in the interval of 0 – 1 seconds. Due to the significant flow rate and pressure drop, the volume of liquid in the tank is quickly depleted and in 1.5 seconds the immediate flow rate of the modified geometry drops below the flow rate of the original geometry. The increase in the total flow rate could also be achieved by increasing the volume of the tank, which is, however, not necessary.

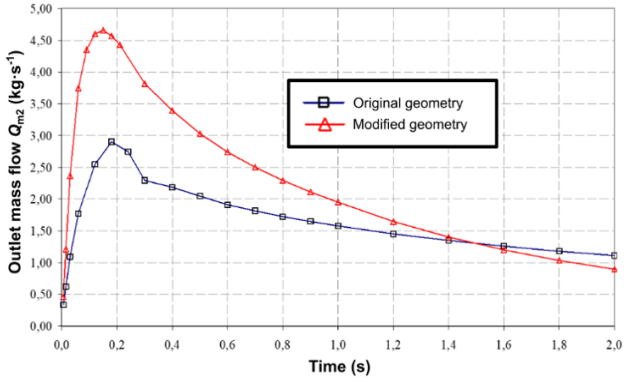


**Figure 10.** Comparison of the original and modified geometry – dependence of the flow rate from the tank on time.

The total amount of liquid flowed in 4 seconds calculated based on the outlet flow rate is 4.96 liters, while the volume flowed in the first second is 2.98 liters of water. At the time of 2 seconds, when the valve starts to close, the volume of liquid flowed is 4.22 liters. Fig. 10 shows the velocity fields for selected opening positions of the modified valve:

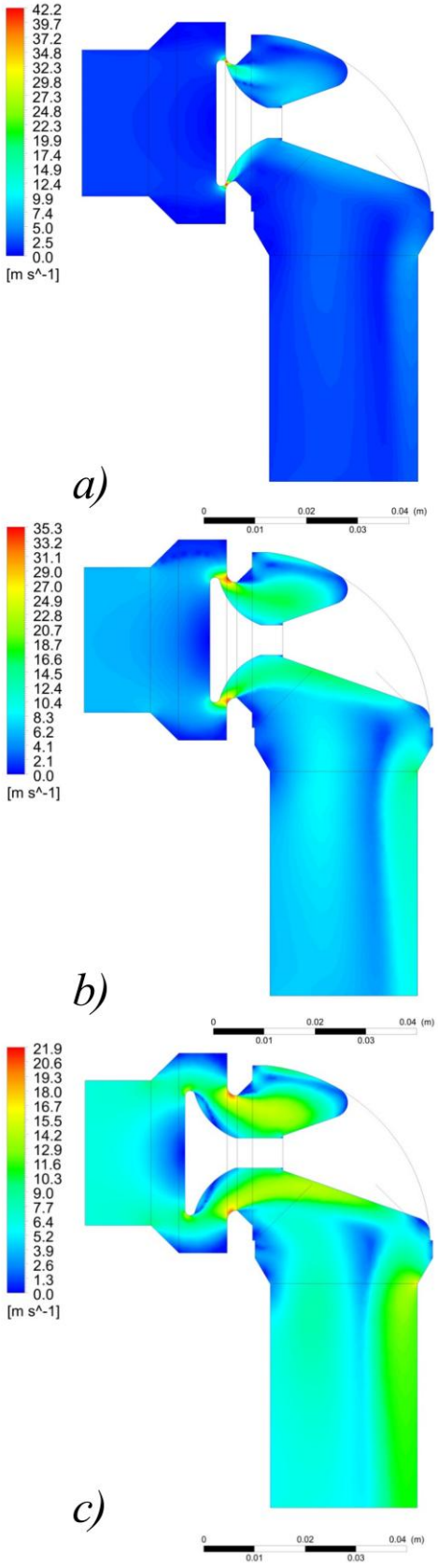


**Figure 11.** Velocity field in the plane of symmetry of the modified geometry when the valve is opened to: a) 0.5 mm; b) 2 mm; c) 7 mm.

Fig. 12 shows the pressure fields in individual selected opening steps of the modified valve geometry.

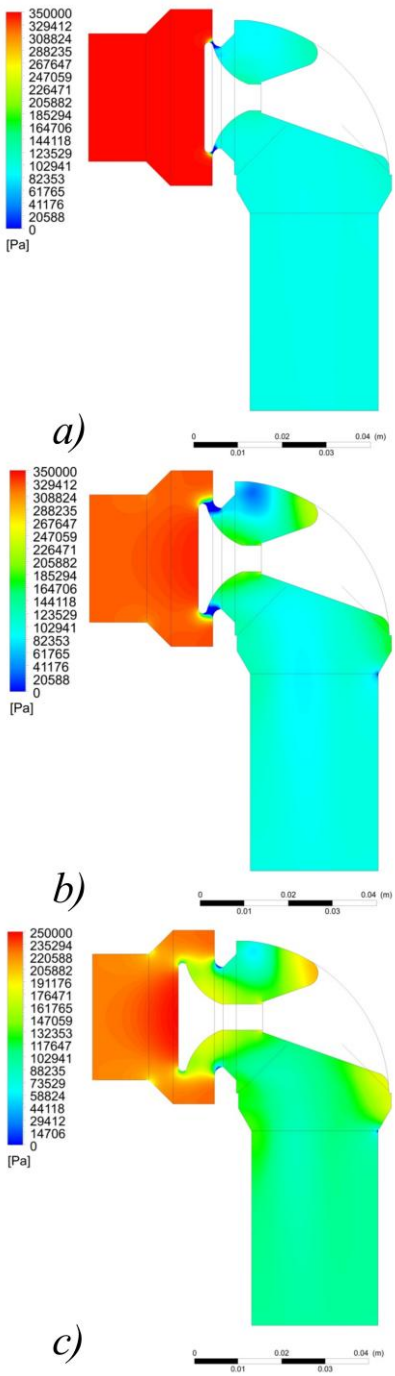


**Figure 12.** Pressure field in the plane of symmetry of the modified geometry when the valve is opened to: a) 0.5 mm; b) 2 mm; c) 7 mm.

## 5 EXPERIMENTAL VERIFICATION

The results of the numerical solution were verified by experimental measurements performed according to the scheme shown in Fig. 13.

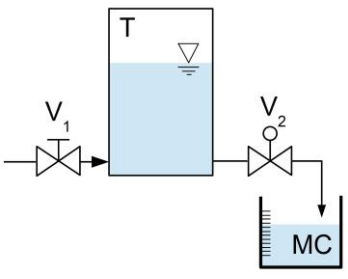


**Figure 13.** Scheme of the experiment.

The inlet flow into the tank (T) is passed through the inlet manual valve $V_1$, which was set so that the inlet flow at atmospheric pressure in the tank reached 0.5 kg·s$^{-1}$. The pressure in front of the valve $V_1$ was reduced to 350 kPa. The valve with modified geometry $V_2$ was opened electronically in accordance with the assumptions in the numerical calculation. For simplicity, the flow rate was not measured, but the total volume of water flowing through the valve $V_2$ for a period of 2 s using a measuring cylinder (MC). Three measurements were made under the same boundary conditions, the results of which are shown in Tab. 3.

| Method | $V_{total}$ (*l*) | $\Delta$ (%) |
|---|---|---|
| Numerical calculation | 4.22 | |
| Experiment 1 | 4.16 | -1.4 |
| Experiment 2 | 4.10 | -2.8 |
| Experiment 3 | 4.11 | -2.6 |

**Table 3.** Measured data of the total volume flowed through the valve in 2 seconds with deviations.

The experimental results confirm good agreement with the numerical calculation, with the measured total water volume showing lower values by an average of 2.27%, which may be caused by manufacturing inaccuracy as well as the roughness of individual valve components.

## 6 CONCLUSION

The results of simulations and calculations within the original geometry of the discharge valve point to obvious design deficiencies. During the operation of the original valve, undesirable cavitation occurred in certain time periods and areas. The original leading edge of the valve guide part caused a sudden change in the flow, which resulted in a decrease in flow rate. The low flow rate was also caused by the valve being extended to a level of up to 10 mm, which reduced the flow cross-section of the valve.

Due to the shortcomings of the original geometry of the discharge valve, design modifications were made to achieve optimal flow properties of the valve. The modification, among other things, also included limiting the maximum distance of the valve extension in the open state to 7 mm to achieve an optimal flow cross-section. The valve design modification based on the calculations achieved an optimal shape in terms of flow and pressure ratios. The improvement achieved in terms of the amount of water flowed during the first second represents approximately 49%, since 2.984 liters of liquid flowed through the modified valve at that time compared to 1.997 liters in the original version. During the first two seconds, when the valve opens and subsequently remains in the open state, the increase in flow compared to the original valve design represents up to 52%, while the total volume of liquid flowed during the same period increased from the original 3.266 liters to 4.22 liters.

The actual volume verified by the experiment shows an average total value of 4.12 liters, which is 2.27% lower than the numerical calculation. Nevertheless, the modified geometry shows a significant increase in the volume of water flowed over a defined period of time compared to the original geometry.


### ACKNOWLEDGMENTS

This work was supported within Project IVG-25-01; by VEGA granting agency within Project No. 1/0224/23, Project

No. 1/0587/25; by KEGA granting agency within Project No. 031TUKE-4/2025.

**REFERENCES**

[Amirante 2016] Amirante, R., et al. Sliding spool design for reducing the actuation forces in direct operated proportional directional valves: Experimental validation. Energy Conversion and Management, July 2016, Vol.119, pp 399-420. ISSN 0196-8904

[Filo 2021] Filo, G., et al. Design and Flow Analysis of an Adjustable Check Valve by Means of CFD Method. Energies, April 2021, Vol.14, No.8, 2237. ISSN 1996-1073

[Frosina 2015] Frosina, E., et al. A mathematical model to analyze the torque caused by fluid-solid interaction on a hydraulic valve. Journal of Fluids Engineering, December 2015, Vol.138, No.6, 061103. ISSN 0098-2202

[Chen 2025] Chen, S., et al. CFD simulation-based flow field analysis and structural optimization of the spool in an electro-hydraulic proportional directional valve. Flow Measurement and Instrumentation, December 2025, Vol.106, 102999. ISSN 0955-5986

[Lecheler 2022] Lecheler, S. Computational Fluid Dynamics. Getting Started Quickly With ANSYS CFX 18 Through Simple Examples. Wiesbaden: Springer, 2022. ISBN 978-3-658-38453-1

[Li 2023] Li, R., et al. Review of the Research on and Optimization of the Flow Force of Hydraulic Spool Valves. Processes, July 2023, Vol.11, No.7, 2183. ISSN 2227-9717

[Olivetti 2020] Olivetti, M., et al. Valve Geometry and Flow Optimization through an Automated DOE Approach. Fluids, January 2020, Vol.5, No.1, 17. ISSN 2311-5521

[Shi 2025] Shi, L., et al. Structural optimization and mechanical property analysis of butterfly valves based on Kriging surrogate model. Building and Environment, September 2025, Vol.283, 113343. ISSN 0360-1323

[Wexler 1976] Wexler, A. Vapor Pressure Formulation for Water in Range 0 to 100 °C. A Revision. Journal of Research of the National Bureau of Standards – A. Physics and Chemistry, July 1976, Vol.80A, No.5, pp 775-785. ISSN 0022-4332

[Yang 2025] Yang, W. CFD-based axial steady-state hydrodynamic study and structural optimization of miniature switching valve. Flow Measurement and Instrumentation, December 2024, Vol.100, 102744. ISSN 0955-5986

**CONTACTS:**

Ing. Ivan Mihalik, PhD.
Technical University of Kosice, Faculty of Mechanical Engineering, Department of Power Engineering
Vysokoskolska 4, Kosice, 042 00, Slovakia
ivan.mihalik@tuke.sk